

Electrocatalysts for the Selective Reduction of Carbon Dioxide to Useful Products

Dan Ren, Yun Huang, and Boon Siang Yeo*

Abstract: The electrochemical reduction of carbon dioxide (CO₂) to hydrocarbons and alcohols holds great promise as a sustainable and green method to produce valuable carbon fuels. In this work, we review the catalysts used in the selective reduction of CO₂ to formate, carbon monoxide, methane and ethylene.

Keywords: Carbon dioxide · Electrocatalysis · Mechanism · Selectivity

1. Introduction

Currently, more than 80% of the world's energy needs are met by burning fossil fuels such as oil or natural gas. The supply of these fuels is intrinsically limited and will eventually run out. Combustion of fossil fuels also generates carbon dioxide (CO₂), which is a suspected accelerant of global warming and a regulatory burden for industrial emitters.^[1] One solution for reducing atmospheric CO₂ is carbon capture and sequestration.^[2] The practicality of this process is however constrained by safety, space and cost. The alternative is to chemically reduce the emitted CO₂ into carboxylic acids, hydrocarbons or alcohols. The advantage of this approach is that some of these products (for example, methane) are already part of our energy infrastructure. Hence, our existing fossil fuels-powered machines do not need to be modified extensively. Hydrocarbon and alcohol fuels, especially if they are liquids, are also more easily stored and transported. If the energy used for the reduction processes is generated from a renewable source such as solar or wind, we could envisage a future fuel production cycle that is closed-loop with net zero carbon emission. CO₂ can also be used as a cheap carbon source for synthesizing bigger organic molecules such as ethylene, which is a valuable chemical feedstock for the polymer industries.

CO₂ reduction can be achieved photocatalytically and electrochemically. Photocatalytic reduction of CO₂ is more

direct, but the conversion, as measured by the quantum yield, is very low.^[3] The electrochemical reduction of CO₂ proceeds more efficaciously, with faradaic efficiencies up to 80–90% under certain conditions.^[4] Considering that the electricity applied for the process can be generated from solar farms and that its price is fast approaching grid parity, an arguably more promising way of converting CO₂ to hydrocarbons and alcohols would be by electrochemical methods.

The electrochemical reduction of CO₂ has been explored using heterogeneous and molecular catalysts under a variety of conditions such as different working potentials and in aqueous, organic and ionic liquids.^[4,5] CO₂ electroreduction using metal electrodes in aqueous electrolytes has been most extensively studied, especially by Y. Hori and co-workers.^[6] The metals tested for CO₂ electroreduction have been traditionally divided into four categories. The first, which consists of metals such as Pb, Cd, Sn and Hg, mainly reduces CO₂ to *OCHO or *COOH, which then undergoes a net one-electron transfer to become formate (HCOO⁻). Metals in the second group (Au, Ag, Zn) have the capability to dissociate *COOH, *via* a single C–O bond scission to give CO, which is liberated from the surface as a gas. The third category of metals (Ni, Fe, Pt, Ti) does not sustainably reduce CO₂. Hydrogen is formed instead. This is likely due to the initial formation of strongly adsorbed CO on the surface, which acts as a poison to inhibit any further CO₂ reduction. Finally, the fourth group which consists of copper metal is known to hydrogenate and even dimerize CO₂ into substantial amounts of hydrocarbons and alcohols.^[5a] To date, copper and its derivatives are the most promising catalysts for reducing CO₂ to methane, ethylene and ethanol, *etc.*

However, problems such as poor selectivity and the need for high overpotentials prevent this process from being commercialized. Jaramillo and co-workers detected at least 16 different products during CO₂ electroreduction on a polycrystalline copper surface (Fig. 1).^[5c] The poor selectivity could be attributed to the variety of reaction sites on the surface and the fact that CO₂ electroreduction on copper is a multistep process with many shared intermediates and reaction pathways.^[7] The selectivity of reaction is also highly susceptible to changes in local pH, temperature and types of electrolytes used.^[4,8] Bond breaking and formation further impose significant kinetic barriers which account for the sizable overpotential needed. Fast deactivation of the Cu catalyst is another serious issue, and usually occurs after several hours of CO₂ reduction.^[9] The loss of activity for CO₂ reduction is believed to originate from amorphous carbon and/or heavy metals deposition on the surface during CO₂ reduction.

In the light of the above considerations, recent works performed in the field of CO₂ electroreduction have focused on the development of robust catalytic systems that have high selectivity towards a certain product at a minimal overpotential. Work has been done to correlate the product distribution with factors such as morphology and chemical composition of the electrodes, CO₂ pressure, reaction temperature and buffer strength/type.^[4,5f,8b,10] Quantum chemical simulations using density functional theory have also been utilized to analyze the underlying mechanism of CO₂ electroreduction.^[7,11] Although these computational models simplify the reaction environment, they nonetheless provide an excellent guide for designing electrocatalysts.

A review summarizing some advances

*Correspondence: Dr. B. S. Yeo
Department of Chemistry
Faculty of Science
National University of Singapore
3 Science Drive 3, Singapore 117543
Tel.: +65 6516 2836
E-mail: chmyeos@nus.edu.sg

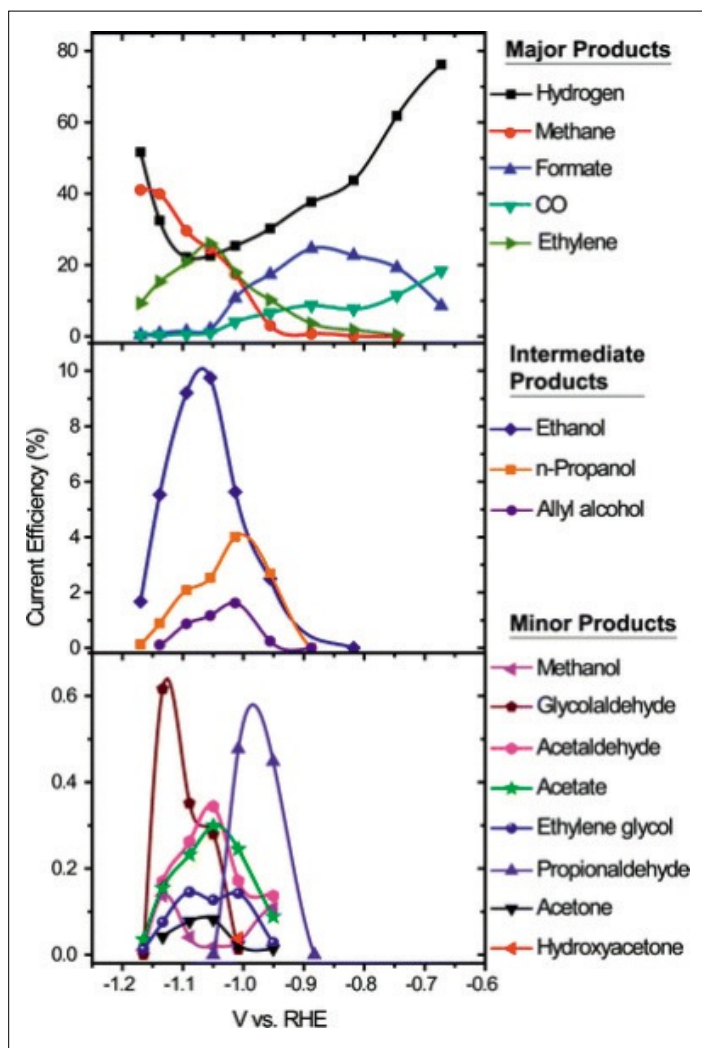
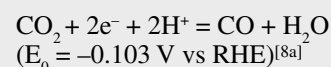


Fig. 1. Faradaic efficiencies for CO_2 electroreduction products formed on polycrystalline copper as a function of potential. Reprinted with permission from ref. [5e]. Copyright © Royal Society of Chemistry.

found to give the best performance. This was attributed to the optimal balance between its surface- CO_2^* intermediate interaction and kinetic activation towards protonation and further reduction. Copper rubeanate metal organic frameworks (CR-MOF) was also recently found to be more efficient and selective than Cu metal in producing HCOO^- from CO_2 reduction.^[17] The onset potential for CO_2 reduction on CR-MOF was 0.2 V more positive compared to that on a Cu metal electrode. Furthermore, the quantity of formate was 13 times larger. The metallic site of CR-MOF is ionic, which is thought to decrease the electron density of Cu. This may lead to weaker adsorption of CO_2 which prevents it from being further reduced, thus giving a higher yield of HCOO^- .

2.2 Carbon Monoxide

The electrochemical half reaction for the formation of carbon monoxide is:



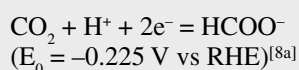
A moderately adsorbed $^*\text{COOH}$ can undergo a single C–O bond scission and protonation to give $^*\text{CO}$ and H_2O . Weakly-bonded $^*\text{CO}$ can then desorb as a gas.^[6] The faradaic efficiencies of CO production during a constant current electrolysis at -5 mA/cm^2 on Au, Ag and Zn in 0.1 M KHCO_3 electrolyte were 87.1, 81.5, 79.4% respectively, while the corresponding potentials were at -1.14 V , -1.37 V , -1.54 V vs. NHE.^[6] The overpotentials for these three metal electrodes to produce CO are therefore 0.6 V, 0.9 V and 1.0 V respectively.^[6] Recently, Kanan and co-workers reported three electrocatalysts that selectively produce CO at very low overpotentials.^[18] They first reported $>50\%$ CO production in CO_2 -saturated 0.5 M NaHCO_3 electrolyte on Sn/SnO_x thin films electrodes at an overpotential of 0.6 V.^[18a] Subsequently, they reported that annealed thick Cu₂O film exhibited 47% CO production in 0.5 M NaHCO_3 with an overpotential of 0.25 V, which is much lower than their Sn/SnO_x thin films.^[18b] Oxide-derived Au nanoparticles, reported by the same group, also exhibit enhanced CO production with faradaic efficiency of 65% at -0.25 V vs RHE and 96% at -0.35 V vs RHE. The overpotentials are therefore respectively 0.15 and 0.25 V.^[18c] All three catalysts are essentially metal oxides that have been reduced to their corresponding metals during the application of cathodic potentials. It was hypothesized that unique surface structures produced during the reduction reaction stabilized the formation of CO_2^* intermediates. This in turn

made in the selective electroreduction of CO_2 to formate, CO, CH_4 and C_2H_4 will be presented. Electrocatalysts consisting of metals, metal oxides and metallic nanostructures, will be grouped according to their selective electroreduction of CO_2 to one particular product. The intention of this review is not to summarize all the works on CO_2 electroreduction. We therefore apologize for some unavoidable omissions. More comprehensive reviews of CO_2 electroreduction can be found in the works of Gattrell *et al.*, Hori *et al.* and Lu *et al.*^[8a,12a,b]

2. Catalysts for Selective CO_2 Reduction

2.1 Formate

The electrochemical half reaction for the formation of formate (HCOO^-) is:



It is widely accepted that CO_2 undergoes proton and electron transfer to give

either $^*\text{COOH}$ or $^*\text{OCHO}$. The intermediate then desorbs as formate after a net one-electron transfer.^[11a,13]

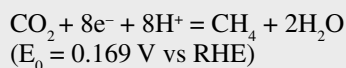
Hori *et al.* studied the electrochemical reduction of CO_2 at different metal electrodes and found that formate is selectively produced on Pb, Hg, In, Sn, Cd and Tl in 0.1 M KHCO_3 .^[6] The faradaic efficiencies range from 78.4 to 99.5%, and the overpotentials required under the tested current density range from 0.85 to 1 V. On Pb metal, Köleli *et al.* reported 90% faradaic efficiency of formate production in 0.5 M KHCO_3 with an overpotential of $\sim 0.6 \text{ V}$ in an electrochemical fixed bed reactor.^[14] Metal oxides have also been explored for CO_2 reduction to formate. Wu *et al.* studied the relationship between the thickness of tin oxide layers and catalytic performance.^[15] The formation of formate was optimized using a 3.5 nm thick SnO_x layer, with a faradaic efficiency of 64% at an overpotential of $\sim 0.4 \text{ V}$. Zhang *et al.* synthesized tin oxide nanocrystals with high surface areas.^[16] This catalyst can produce formate at overpotentials as low as 0.34 V. When supported on graphene, the faradaic efficiency of formate can reach $>93\%$ at an overpotential of 1.1 V. 5 nm-sized tin oxide particles were also

lowers the overpotentials required for the formation for CO. A clear description of the nature of these catalytic sites by nano-spectroscopy or microscopy would aid in further improvements of these catalysts.

Lu *et al.* recently reported a dealloyed process to produce nanoporous Ag (np-Ag) with a unique monolithic and curved inner structure (Fig. 2A). This catalyst exhibited excellent CO₂ electroreduction to CO with a faradaic efficiency of 79% at -0.4 V vs RHE and 90% at -0.5 V vs RHE in 0.5 M KHCO₃ (Fig. 2B–D).^[19] This exceptional activity could be attributed to the highly curved surface of the np-Ag catalyst which may contain a high density of step sites and higher-index facets. These features could improve the surface migration of the hydrogen donor HCO₃⁻ to the surface sites in the interior of the np-Ag, which is considered to be rate-determining by the authors.

2.3 Methane and Ethylene

The electrochemical half reactions for the formation of methane (CH₄) and ethylene (C₂H₄) are:



CO₂ electroreduction to these two products transpire on polycrystalline Cu surfaces, albeit with the simultaneous production of many other compounds like HCOO⁻, CO, C₂H₅OH, *etc.* (Fig. 1).^[4,5e] The poor selectivity can be attributed to the heterogeneity of catalytic sites on the polycrystalline Cu. A highly impactful work to tune the selectivity of CH₄ and C₂H₄ was first performed by Hori and co-workers.^[20] They studied the distribution of products formed on copper single crystals surfaces during CO₂ electroreduction at -5 mA/cm² in 0.1 M KHCO₃.^[20b] Cu(111) and Cu(100) were respectively found to be more selective for CH₄ and C₂H₄ formation. Interestingly, the selectivity could be tuned by introducing atomic steps on these surfaces (brought about by cleaving the single crystal substrates at specific angles). As an illustration, CO₂ reduction on Cu(100) produced C₂H₄ and CH₄ with faradaic efficiencies of 40.4 and 30.4% respectively, thus giving a C₂H₄/CH₄ ratio of 1.3. The selectivity towards C₂H₄ could be enhanced by using a Cu(711) surface which consisted of four atomic rows of (100) terrace and one atomic height of (111) steps. This catalyst reduced CO₂ with far-

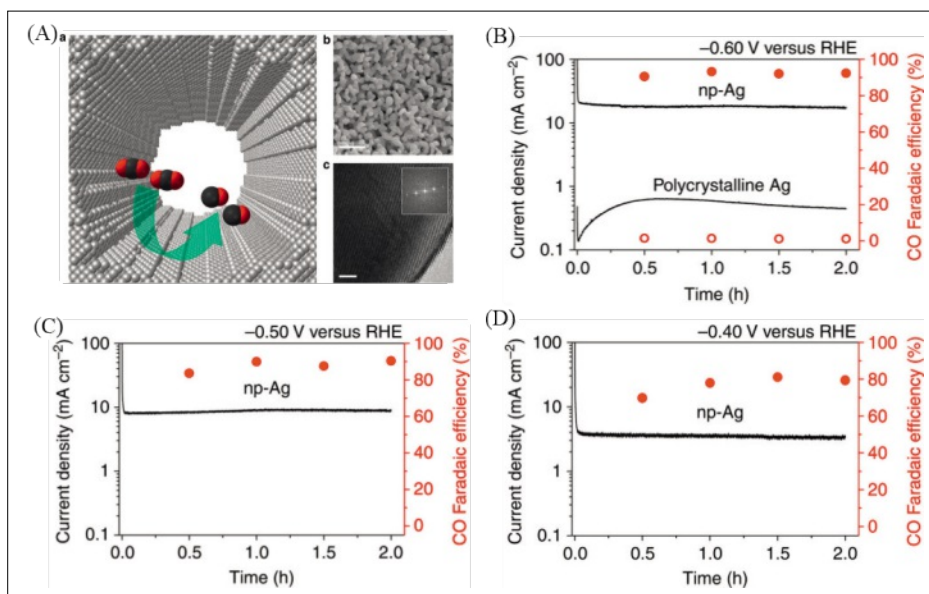


Fig. 2. (A) (a) Schematic diagram of the interior of a nanoporous Ag (np-Ag) catalyst, (b) SEM image of np-Ag dealloyed in 5 wt% HCl for 15 min and further in 1 wt% HCl for 30 min, (c) corresponding HR-TEM image (scale bar, 2 nm). CO₂ electroreduction activity of np-Ag and polycrystalline silver at (B) -0.60 V, (C) -0.50 V and (D) -0.40 V vs. RHE. Adapted with permission from ref. [19]. Copyright © Nature Publisher Group.

daic efficiencies of 50.0% C₂H₄ and 5.0% CH₄.^[20a] A much higher C₂H₄/CH₄ ratio of 10 was thus achieved! A ‘volcano’-like plot was also obtained when the C₂H₄/CH₄ ratio was plotted against the angle of the crystal orientation with reference to Cu(100) (Fig. 3). This trend suggests that an optimum density of atomic steps on the terraces is an important factor in enhancing the formation of C₂H₄ during CO₂ reduction.

Roughened Cu surfaces have also been found to exhibit enhanced selectivity towards C₂H₄ formation. Tang *et al.* reported that a Cu surface deposited with roughened Cu nanoparticles reduced CO₂ at -1.1 V vs RHE in 0.1 M KClO₄ electrolyte with faradaic efficiencies of 36 and ~1 % for C₂H₄ and CH₄ respectively (Fig. 4).^[5f] The

selectivity towards ethylene is considerably higher compared to that observed on electrochemically polished and Argon ions (Ar⁺) sputtered Cu surfaces. With the assistance of quantum chemical simulations, it was proposed that a greater surface population of undercoordinated sites on the Cu nanoparticles would favor the buildup of a high coverage of HO* intermediates. This would in turn favor the formation rate of C₂H₄.

Inspired by these studies, our group prepared Cu mesocrystal catalysts by the *in situ* reduction of a CuCl film during CO₂ reduction.^[21] This material was shown to reduce CO₂ at -0.99 V vs RHE to produce C₂H₄ and CH₄ at faradaic efficiencies of 27.2 and 1.47% respectively. A

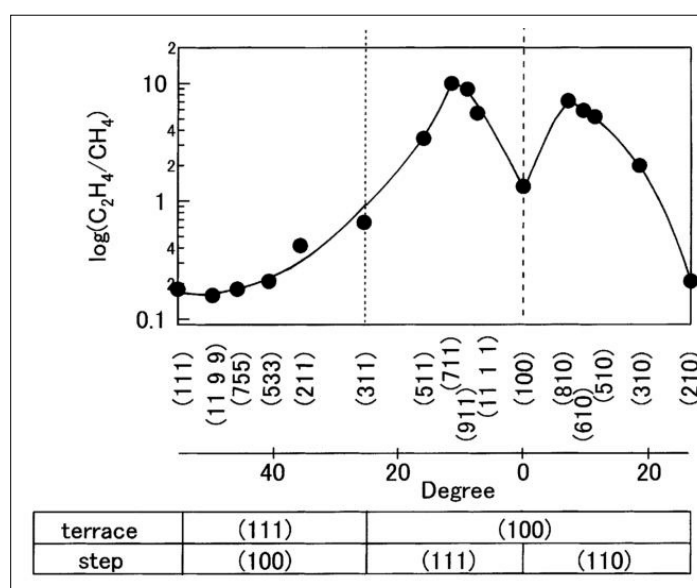


Fig. 3. Plot of log(C₂H₄/CH₄) value vs. the angle of Cu crystal orientation. The figure is separated into three parts by two dash lines. Left: (111) terrace plus (100) terrace plus (111) steps; Middle: (100) terrace plus (111) steps; Right: (100) terrace plus (110) steps. Reprinted with permission from ref. [20a]. Copyright © Elsevier.

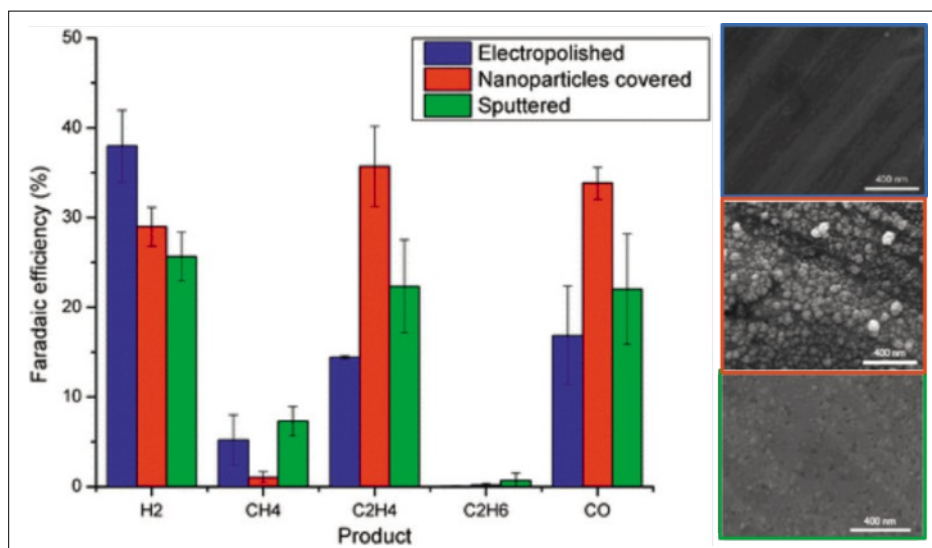


Fig. 4. Faradaic efficiencies for CO₂ electroreduction products on three catalyst surfaces in CO₂-saturated 0.1 M KClO₄ at -1.1 V vs RHE. These are electropolished Cu surface (in blue), copper nanoparticles covered surface (in red) and sputtered surface (in green). SEM images of the three catalysts are shown on the right hand side. Reprinted from ref. [5f]. Copyright © Royal Society of Chemistry.

C₂H₄/CH₄ ratio of ~18 was thus achieved (Fig. 5). In contrast, an electropolished Cu surface and Cu nanoparticles formed by pulse electrodeposition exhibited C₂H₄/CH₄ ratios of only 3.1 and 2.3 respectively. The formation and characterization of the Cu mesocrystals is shown in Fig. 6. CuCl was first electrodeposited on a pristine Cu electrode (Fig. 6A,B). X-ray diffraction (XRD) and X-ray photoelectron spectroscopy (XPS) demonstrated the presence of CuCl (Fig. 6C,D). Then, the sample was used as catalyst for CO₂ reduction. Within a few hundred seconds into the reduction process, well-defined cuboids decorated with numerous particles were observed (Fig. 6E–H). These, termed by us as Cu mesocrystals, were confirmed by XRD and XPS to be metallic Cu. High-resolution transmission electron microscopy (HRTEM) revealed that these catalysts consisted of both Cu(100) terraces and steps (Fig. 6I–L). These features were not observed on either the electropolished Cu or Cu nanoparticles.^[21] For the latter catalyst, HRTEM revealed that their surfaces were smoothly graded, possibly with many steps, but no terraces could be found. This surface was thus classified as a high indexed plane with many steps but with no terraces. Based on these observations and consistent with the work of Hori, we conclude that both Cu(100) terraces and steps are important in enhancing the selectivity of C₂H₄ formation. An industrially relevant feature of the Cu mesocrystals is their excellent activity and selectivity towards C₂H₄ production for at least six hours.

Based on these works, the selective CO₂ electroreduction to C₂H₄ over rough Cu surfaces has been attributed to the presence of steps, edges, defects and specific

crystal planes. It could be posited that a ‘right’ combination of these features was required for optimal C₂H₄ production. In addition to this, Kas *et al.* recently demonstrated that an electrode covered with Cu nanoparticles could yield predominantly either CH₄ or C₂H₄ by changing the concentration of the electrolyte or CO₂ pressure.^[8b] It was suggested that C₂H₄ formation is favored by a high local pH at the interface of the electrode, which could be actualized by lowering the concentration of the electrolyte (hence, affecting its buffer capacity). This study shows that local pH is an important factor that needs to be considered when performing selective CO₂ electroreduction to C₂H₄.

The mechanisms for the formation of CH₄ and C₂H₄ have been proposed. It is widely accepted that CH₄ is formed from adsorbed *CO species.^[11b,13,22] *CO is first protonated/reduced to *CHO. This intermediate is further reduced to *CH₃, and

then to CH₄.^[22b] Hori *et al.* suggested two routes to the formation of C₂H₄.^[23] The first is a Fischer-Tropsch like reaction: insertion of *CO into *CH₂ to give *CH₂CO, which is further reduced to C₂H₄. The second is the direct dimerization of two *CH₂ to give C₂H₄.^[23] Koper *et al.* suggested two possible reaction pathways for C₂H₄ formation on Cu single crystal surfaces.^[22c] One pathway shares an intermediate with the formation of CH₄ and occurs favorably on Cu(111) facets or steps. The other one takes place at Cu(100) facets at relatively low overpotentials. It was proposed that the dimerization of two *CO to give a CO dimer is key in this mechanism. Montoya *et al.* studied the C–C coupling process in CO₂ electrochemical reduction by DFT.^[7] The kinetic energy barriers to C–C coupling was found to decrease significantly with the degree of hydrogenation of C₁ reactants. The more protonated the C₁ species are, the more favored the dimerization would be. More experimental studies are needed to identify the pertinent reaction intermediates so as to ascertain the C–C coupling mechanism during the formation of C₂H₄.

3. Summary

Extensive research has been dedicated to this field of CO₂ electroreduction over the past few years. Progress has been made in both identifying electrocatalysts for selective production of formate, CO and hydrocarbons, and understanding the reaction mechanism. For a more efficient development of efficacious CO₂ reduction catalysts, a deeper characterization of the reaction mechanism and active catalytic sites at the molecular level is needed. Correlations could then be drawn between the properties of the catalysts with the type, lifetime and quantity of transient surface intermediates and products formed during CO₂ reduction. Various state of the

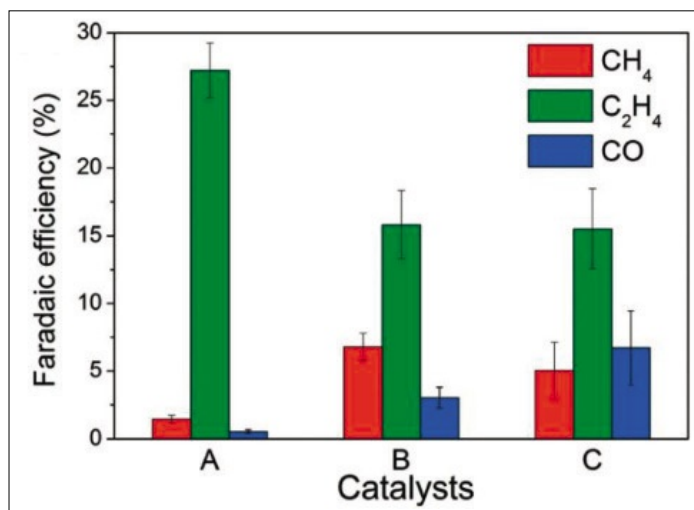


Fig. 5. Faradaic efficiencies of CO₂ electroreduction products (CH₄, C₂H₄ and CO) on catalysts: A = Cu mesocrystals, B = Cu nanoparticles and C = electropolished Cu. Adapted with permission from ref. [21]. Copyright © Royal Society of Chemistry.

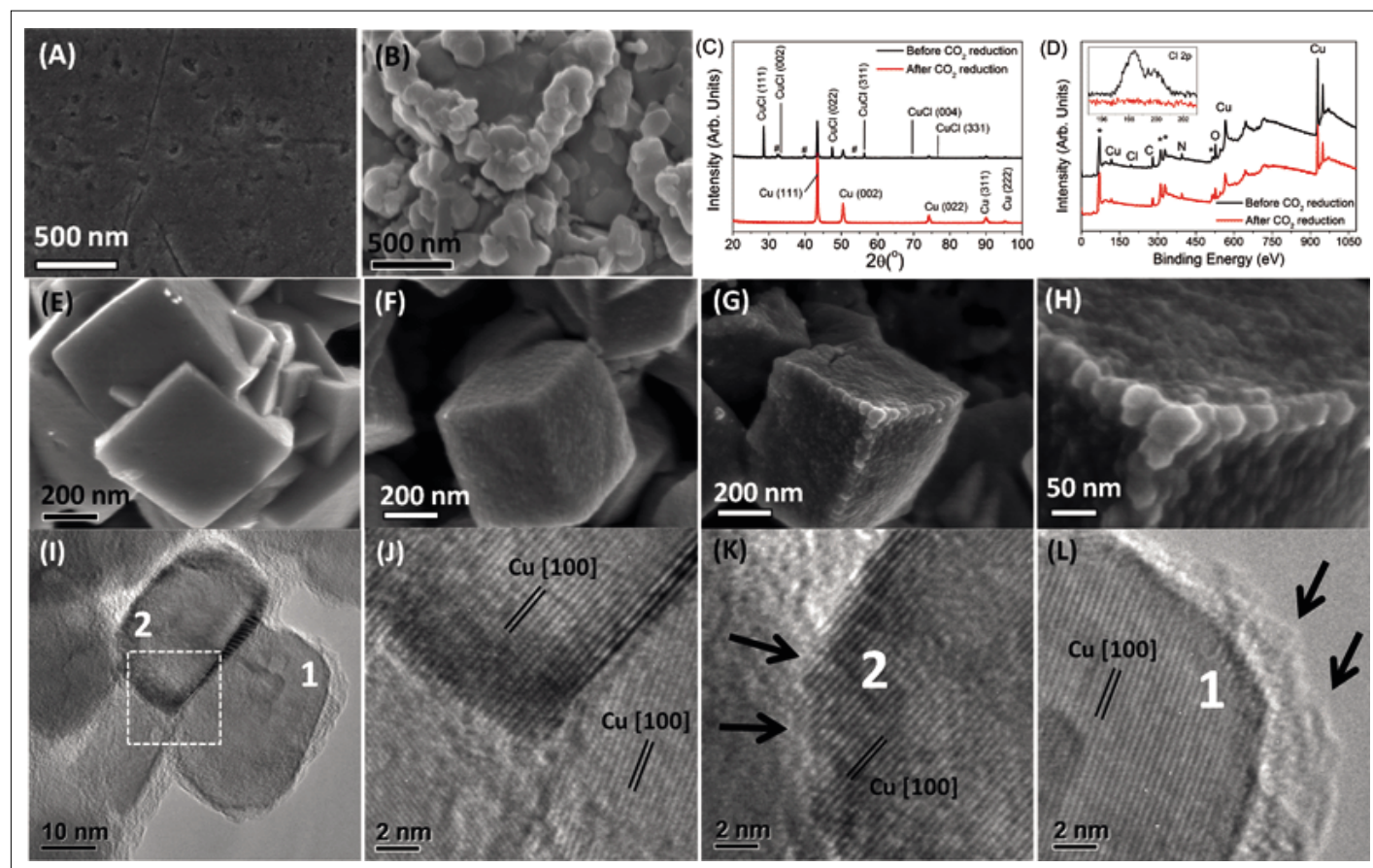


Fig. 6. SEM images of (A) polished Cu and (B) deposited CuCl layer before CO_2 reduction. (C) XRD and (D) XPS data for CuCl layers before (in black) and after 4200 seconds of CO_2 reduction (in red). Time-resolved *ex situ* SEM images showing the formation of Cu mesocrystals after (E) 10, (F) 100, and (G–H) 4200 seconds of CO_2 electroreduction. (I–L) HRTEM images of Cu mesocrystals in (G–H) under increasing magnifications. Steps and edges present on the Cu mesocrystals are indicated by the arrows. Reprinted with permission from ref. [21]. Copyright © Royal Society of Chemistry.

art analytical techniques such as *in situ* time-resolved spectroscopy and electron microscopy could be used for this purpose.

Acknowledgements

This work is supported by a start-up grant (R143-000-515-133) and an academic research fund (R-143-000-587-112) from the National University of Singapore.

Received: January 29, 2015

- [1] T. Stocker, D. Qin, G. Plattner, M. Tignor, S. Allen, J. Boschung, A. Nauels, Y. Xia, B. Bex, B. Midgley, 'IPCC 2013: Climate change 2013: The Physical Science Basis. Contribution of working group I to the fifth assessment report of the intergovernmental panel on climate change', **2013**.
- [2] D. P. Schrag, *Science* **2007**, *315*, 812.
- [3] S. C. Roy, O. K. Varghese, M. Paulose, C. A. Grimes, *ACS Nano* **2010**, *4*, 1259.
- [4] Y. Hori, A. Murata, R. Takahashi, *J. Chem. Soc., Faraday Trans. 1* **1989**, *85*, 2309.
- [5] (a) Y. Hori, K. Kikuchi, S. Suzuki, *Chem. Lett.* **1985**, 1695; (b) K. W. Frese, *J. Electrochem. Soc.* **1991**, *138*, 3338; (c) M. Watanabe, M. Shibata, A. Kato, M. Azuma, T. Sakata, *J. Electrochem. Soc.* **1991**, *138*, 3382; (d) M. Schwartz, R. L. Cook, V. M. Kehoe, R. C. MacDuff, J. Patel, A. F. Sammells, *J. Electrochem. Soc.* **1993**, *140*, 614; (e) K. P. Kuhl, E. R. Cave, D. N. Abram, T. F. Jaramillo, *Energy Environ. Sci.* **2012**, *5*, 7050; (f) W. Tang, A. A. Peterson, A. S. Varela, Z. P. Jovanov, L. Bech, W. J. Durand, S. Dahl, J. K. Nørskov, I. Chorkendorff, *Phys. Chem. Chem. Phys.* **2012**, *14*, 76.
- [6] Y. Hori, H. Wakebe, T. Tsukamoto, O. Koga, *Electrochim. Acta* **1994**, *39*, 1833.
- [7] J. H. Montoya, A. A. Peterson, J. K. Nørskov, *ChemCatChem* **2013**, *5*, 737.
- [8] (a) M. Gattrell, N. Gupta, A. Co, *J. Electroanal. Chem.* **2006**, *594*, 1; (b) R. Kas, R. Kortlever, H. Yilmaz, M. T. M. Koper, G. Mul, *ChemElectroChem* **2014**, DOI: 10.1002/celec.201402373.
- [9] (a) D. W. DeWulf, T. Jin, A. J. Bard, *J. Electrochem. Soc.* **1989**, *136*, 1686; (b) Y. Hori, H. Konishi, T. Futamura, A. Murata, O. Koga, H. Sakurai, K. Oguma, *Electrochim. Acta* **2005**, *50*, 5354.
- [10] (a) S. Sen, D. Liu, G. T. R. Palmore, *ACS Catal.* **2014**, *4*, 3091; (b) H. Yano, T. Tanaka, M. Nakayama, K. Ogura, *J. Electroanal. Chem.* **2004**, *565*, 287; (c) M. Azuma, K. Hashimoto, M. Hiramoto, M. Watanabe, T. Sakata, *J. Electroanal. Chem.* **1989**, *260*, 441; (d) R. Reske, H. Mistry, F. Behafarid, B. Roldan Cuenya, P. Strasser, *J. Am. Chem. Soc.* **2014**, *136*, 6978; (e) O. A. Baturina, Q. Lu, M. A. Padilla, L. Xin, W. Li, A. Serov, K. Artyushkova, P. Atanassov, F. Xu, A. Epshiteyn, T. Brintlinger, M. Schuette, G. E. Collins, *ACS Catal.* **2014**, *4*, 3682.
- [11] (a) A. A. Peterson, F. Abild-Pedersen, F. Studt, J. Rossmeisl, J. K. Nørskov, *Energy Environ. Sci.* **2010**, *3*, 1311; (b) A. A. Peterson, J. K. Nørskov, *J. Phys. Chem. Lett.* **2012**, *3*, 251.
- [12] (a) Y. Hori, in 'Modern Aspects of Electrochemistry', Eds. C. Vayenas, R. White, M. Gamboa-Aldeco, Springer New York, **2008**, Vol. 42; (b) Q. Lu, J. Rosen, F. Jiao, *ChemCatChem* **2014**, *7*, 38.
- [13] T. Hatsukade, K. P. Kuhl, E. R. Cave, D. N. Abram, T. F. Jaramillo, *Phys. Chem. Chem. Phys.* **2014**, *16*, 13814.
- [14] F. Köleli, T. Atilan, N. Palamut, A. M. Gizir, R. Aydin, C. H. Hamann, *J. Appl. Electrochem.* **2003**, *33*, 447.
- [15] J. Wu, F. G. Risalvato, S. Ma, X.-D. Zhou, *J. Mat. Chem. A* **2014**, *2*, 1647.
- [16] S. Zhang, P. Kang, T. J. Meyer, *J. Am. Chem. Soc.* **2014**, *136*, 1734.
- [17] R. Hinogami, S. Yotsuhashi, M. Deguchi, Y. Zenitani, H. Hashiba, Y. Yamada, *ECS Electrochem. Lett.* **2012**, *1*, H17.
- [18] (a) Y. Chen, M. W. Kanan, *J. Am. Chem. Soc.* **2012**, *134*, 1986; (b) C. W. Li, M. W. Kanan, *J. Am. Chem. Soc.* **2012**, *134*, 7231; (c) Y. Chen, C. W. Li, M. W. Kanan, *J. Am. Chem. Soc.* **2012**, *134*, 19969.
- [19] Q. Lu, J. Rosen, Y. Zhou, G. S. Hutchings, Y. C. Kimmel, J. G. Chen, F. Jiao, *Nat. Commun.* **2014**, *5*, 3242.
- [20] (a) Y. Hori, I. Takahashi, O. Koga, N. Hoshi, *J. Mol. Catal. A: Chem.* **2003**, *199*, 39; (b) Y. Hori, I. Takahashi, O. Koga, N. Hoshi, *J. Phys. Chem. B* **2002**, *106*, 15.
- [21] C. S. Chen, A. D. Handoko, J. H. Wan, L. Ma, D. Ren, B. S. Yeo, *Catal. Sci. Technol.* **2015**, *5*, 161.
- [22] (a) Y. Hori, A. Murata, Y. Yoshinami, *J. Chem. Soc., Faraday Trans.* **1991**, *87*, 125; (b) K. Schouten, Y. Kwon, C. Van der Ham, Z. Qin, M. Koper, *Chem. Sci.* **2011**, *2*, 1902; (c) K. J. P. Schouten, Z. Qin, E. P. Gallent, M. T. M. Koper, *J. Am. Chem. Soc.* **2012**, *134*, 9864.
- [23] Y. Hori, R. Takahashi, Y. Yoshinami, A. Murata, *J. Phys. Chem. B* **1997**, *101*, 7075.